Fibers and Polymers 2017, Vol.18, No.11, 2135-2145
DOI 10.1007/s12221-017-7368-4

ISSN 1229-9197 (print version)
ISSN 1875-0052 (electronic version)

Electrospun PU-PEG and PU-PC Hybrid Scaffolds for Vascular Tissue Engineering

Zeynep Karahaliloğlu*

Department of Biology, Faculty of Science and Arts, Aksaray University, Aksaray 68100, Turkey
(Received April 19, 2017; Revised August 6, 2017; Accepted August 9, 2017)

Abstract: Produced via electrospinning, polyurethane (PU) scaffolds have always attracted the interest of medical applications due of their unique properties such as good adhesion, biocompatibility and excellent mechanical strength. However, the poor hydrophilicity and hemocompatibility of PU presented a problem during PU's application in the manufacturing of biomedical materials. We hypothesized that the incorporation of polyethylene glycol (PEG) and phosphatidylcholine (PC) into electrospinning solution of PU could improve the cell affinity and hemocompatibility. This research focused on fabricating hybrid PU-PEG and PU-PC random/aligned scaffolds through electrospinning technique and comparing their properties as a potential biocompatible scaffold for vascular tissue engineering. PC was doped into a PU solution in order to prepare an electrospun scaffold through the electrospinning technology while crosslinked electrospun PU-PEG hybrid scaffolds were fabricated by photoinduced polymerization. The contact angle dramatically decreased from 122.3±0.8 ° to 39.1±0.8 ° with doping of PC in electrospinning solution while it decreased from 122.3±0.8 ° to 41.6±0.8 ° with doping of PEG. Furthermore, the mechanical properties of PU scaffolds were altered significantly by the addition of PC. The hemolysis and cytocompatibility assays demonstrated that these composite scaffolds could potentially be used as a small-diameter vascular graft.

Keywords: Electrospinning, Nanofibers, Polyurethane, Poly(ethylene glycol) (PEG), Phosphatidylcholine (PC)

Introduction

Cardiovascular diseases are the largest contributor to global mortality around the world and the latest global heart disease statistics predict the number of deaths caused by heart disease to reach to 23.6 million in 2030 while 17.3 million people died due to cardiovascular related reasons in 2008 [1,2]. Recently, a growing number of researchers in the vascular tissue engineering community have focused on solving problems associated with small diameter grafts such as thrombogenicity, mechanical incapability and anticoagulant related haemorrhage. Thus, finding a material alternative to conventional graft materials has become a major focus attention.

Expanded polytetrafluoroethylene (PTFE) and Dacron (polyethylene terephthalate, PET) have been routinely used for small diameter vascular grafts applications and they are ascribed as standard biomaterial between prosthetic vascular grafts. Although these materials have proven to perform well in a large diameter vessel (>5 mm), they show limited capability in smaller diameter [3,4]. Additionally, PTFE or PET in small diameter blood vessel applications causes several complications like aneurysm, intimal hyperplasia, calcification, thrombosis and infection [5,6]. These drawbacks create a need to fabricate a novel biologically viable vascular substitute for small-diameter vascular grafting. Polyurethanes (PURs) are broad family polymers, which have been studied extensively in various scaffolds applications [7]. They are extremely interesting due to their properties such as good processability, high elongation and excellent resistance and have attracted interest and considerable attention in recent years as potential small-diameter vascular graft material [8]. Medical grade TPU has good biocompatibility as a blood vessel graft [9] and electrospun polyurethanes are a potential biomaterial for blood vessel replacement with excellent mechanical properties such as porosity, strength and very high extensibility [10,11].

Various approaches to design the vascular scaffold have been studied and among these, the mimicking of the three-dimensional extracellular matrix using nanoarchitecture has recently been paid attention, i.e. electrospinning. Electrospinning is an interesting approach to produce fibrous small diameter polymeric vascular grafts with mechanical properties comparable to native vascular tissue [12,13]. Electrospinning process is based on drawing of a polymeric solution across an electric field and solidification of nanofibrillar structures on a rotating or stable collector [14,15]. The electrospun fibers can be organized in the form of nonwoven or oriented mesh depending on the used collector type. For example, bilayered tubes as vascular graft material or axially aligned nanofibrous tubes for blood vessels, nerve conduits and ligaments as they are prepared by researchers in the required format [16,17]. It is reported that aligned topography has a superiority, which it displays through mimicking the anisotropic microstructure of native vascular tissue, regulating the mechanical properties or improving vascular tissue regeneration [18,19]. Surface composition plays a key role in stimulating cellular interactions between cells and scaffolds as well as surface topography. The addition of biocompatible additives have shown promising superior attributes compared with polymers alone

*Corresponding author: mitokonri@gmail.com

in the field of biomedical materials. These additives such as poly(ethylene glycol) (PEG), hydroxyapatite (HA), phosphatidylcholine (PC) or gelatin improve the mechanical properties, hydrophilicity, biocompatibility or hemocompatibility. PEG has a large number of hydrophilic groups on its surface and the hydrophilicity of the scaffolds is increased by the incorporation of a hydrophilic polymer into the electrospinning solution. For example, Wang *et al*. reported that a small-diameter vascular graft from polyurethane and poly ethylene glycol solutions (to prepare a PU/PEG blend with different weight ratios) was fabricated by electrospinning. The researchers selected PEG to improve the hydrophilicity and hemocompatibility of the grafts and they were characterized biologically and mechanically [20]. They showed in another study that the crosslinked PU/PEGMA nanofibers produced by electrospinning had great potential as a vascular graft [21].

Modification of the biomaterial surface using phosphatidylcholine (PC) is a growing interest in tissue engineering applications because of excellent hemocompatibility of PC head groups [22]. Phosphatidylcholine (lecithin) is a phospholipid, which is a major constituent of nervous and brain tissue. It has good biocompatibility and capability of mixing with various types of polymers such as poly(lactic-co-glycolic acid) (PLGA), poly(lactic acid) (PLA), poly-epsilon- caprolactone (PCL) and poly-L-lactic acid (PLLA) [23-25]. Cao *et al.* reported the synthesis of novel polyurethane synthesized by chain-extension of biodegradable poly(L-lactide) functionalized phosphatidylcholine (PC) with hexamethylene diisocyanate (HDI) as chain extender (PUR-PC). Preliminary results have shown that this novel polyurethane was better compared to the traditional counterpart due to its great hemocompatibility and hydrophilicity [26]. Nirmala *et al.* reported lecithin-blended polyamide-6 nanofibers produced via electrospinning technique for human osteoblastic (HOB) cell culture applications. The analysis results demonstrated that the electrospun polyamid-6/lecithin nanofiber was a cell-compatible material and had a potential for biomedical applications [27].

This paper focused on fabricating PU-PEG and PU-PC composite fibrous small-diameter vascular graft using the electrospinning technique. Considering the advantages of PEG and PC, the fantastic property of electrospun polyurethane in preparation of small-diameter vascular graft, the structure and cell/blood response of PU-PEG or PU-PC composite fibrous scaffolds were investigated in detail. Furthermore, to date, there is no report dealing with polyurethane/lecithin-blended nanofibers, which has looked into their feature in small-diameter vascular graft applications. The bare and composite PU scaffolds in the form of the randomly-oriented and aligned were prepared and mechanical, morphological and chemical properties were evaluated by tensile test machine, scanning electron microscopy (SEM) and fourier transform infrared spectroscopy (FTIR), respectively. The effect of both a surface topography and a surface chemistry on hemocompatibility and biocompatibility of PU scaffolds were comparatively studied using human umbilical vein endothelial cell line (HUVECs) to verify their capability to be used in vascular scaffold applications.

Experimental

Materials

Polyurethane elastomer granulate, Elastollan® 1185A (polyether type polyurethane elastomer) was provided by BASF GmbH (Germany). Polyethylene glycol (PEG) (Mw= 300 Da) and phosphatidylcholine (PC, lyophilized powder), N,N'-Methylenebisacrylamide (MBAm) and benzophenone (BP) were received from Sigma Aldrich (USA). PEG1000 (Mw=1000) were used for the fabrication of scaffolds.

Dulbecco's modified Eagle's medium (DMEM), fetal bovine serum (FBS), penicillin-streptomycin, L-glutamine and trypsin-EDTA were purchased from Biological Industries (Israel). Live/dead cell double staining kit was obtained from Sigma-Aldrich (USA).

Scaffold Preparation

PU was dissolved in THF (tetrahydrofuran)/DMF (dimethylformamide) solutions (1:1 v/v) at 10 % (w/v) concentration overnight. Electrospinning instrument included a high voltage DC power supply (Spellman CZE1000R), syringe pump and two types collector i.e. rotating-drum and plate collector type. The bare PU solution was electrospun at an applied voltage of 20 kV, a distance between the tip of the syringe and collector of 15 cm and at a rate of 0.2 m*l*/h flow rate during 8 hours. A rotating drum at a speed of 600 rpm were used in the production of the aligned nanofiber scaffolds. The experiment was performed at room temperature (~25 °C) and a relative humidity of ~60 %.

Firstly, in order to prepare the PU-PC composite nanofiber scaffolds, PU was dissolved in the mixture solvent of DMF and THF as the above-mentioned and then PU solution was mixed with phosphatidylcholine (lyophilized form) in a ratio of 1:2 w/w (PC/PU) and the mixture was vortexed to completely dissolve PC in THF/DMF. The solution was electrospun at a voltage of 22 kV, a distance of 15 cm, a flow rate of 0.01 m*l*/h and at room temperature (~25 °C) and a relative humidity of ~60 % during 3 hours. For preparation of PU/PEG composite nanofiber scaffolds, firstly, a mixture of PEG, MBAm as crosslinker and BP as photoinitiator was prepared with the following weight ratio PEG:MBAm:BP [97.5:2.0:0.5 (wt%)]. Then, PU solution (10 wt%) was mixed with above-mentioned mixture, in a ratio of 1:4 w/w (PU/PEG) and the solution was vortexed to obtain a completely homogeneous solution. About 5 m*l* of the polymer solution was placed in the syringe. The tip was positively charged by the generator and the electrospinning process was started. The solutions of PU-PEG were electrospun at a 15-cm working distance and at a 23 kV-applied voltages under UV-

irradation. The process was halted after about 1 hour.

Characterizations

The morphology of electrospun nanofibrous scaffolds was observed using scanning electron microscopy (SEM, JEOL JSM700F). The samples were mounted on Al stages and sputtered with Au/Pt for 5 min. SEM images were collected with an accelerating voltage at 15 kV. The average fiber diameter was analyzed with image-processing software (ImageJ, NIST) by measuring diameters of fibers at 250 points from approximately 5 images taken per area.

The chemical structures of the bare and composite PU nanofiber scaffolds were characterized using an attenuated total reflectance Fourier transform (ATR-FTIR) spectrophotometer (Perkin Elmer, Spectrum Nicolet 520). Each spectrum was acquired with a resolution of 4 cm^{-1} and a wavenumber range of 4000-600 cm^{-1}.

Tensile measurements were conducted on a Universal testing machine (Zwick, 250 kN, USA) using a 100 N load cell. Electrospun bare and composite PU scaffolds with size of 3.0×0.3 cm were tested at a tensile speed of 10 mm min^{-1}. Each sample was tested 6 times and the average results with standard deviation were presented. *E* modulus was calculated from the slope of the stress-strain curves.

Surface wettability is an important factor for biomaterials related to cell attachment, proliferation, migration and viability of cells. The wettability of electrospun bare and composite PU scaffolds was evaluated by contact angle measurements (DSA100, KRUSS, Germany). The samples were cut into 0.5 cm×0.5 cm (length×width) for the analysis and the water droplet images onto the nanofibrous PU samples at an equilibrium state were taken using a viewing software at room temperature. Average static contact angles and the standard deviation of bare and composite PU scaffolds were calculated by obtaining five measurements for each sample.

3-(4,5-di-methylthiazol-2-yl)-2,5-diphenyltetrazolium bromide (MTT) Assay

MTT colorimetric assay was used to determine cell viability and cell proliferation. In this study, cell proliferation on PU nanofiber scaffolds was measured by MTT solution (5 μg/m*l*, diluted with RPMI 1640 without phenol red) and the number of cells in the nanofiber scaffold was compared with tissue culture plates (TCP). The HUVECs were maintained in DMEM supplemented with 10 % FBS and 1 % penicillin-streptomycin and l-glutamine at 37 °C in a 5 % CO_2 incubator until confluency. The cells were harvested by tryspin/EDTA treatment from the cell culture flask and the cells were counted using a hemocytometer. Following the sterilization of the PU nanofibrous scaffolds using 70 % v/v ethyl alcohol, the scaffolds were incubated in 24-well tissue culture plates with HUVECs at a density of 9×10^3 cells/well for 1, 3, 5 and 7 days at 37 °C in 5 % CO_2 incubator for comparisons of control, random and aligned PU nanofibrous scaffolds. The scaffolds were transferred to a new 24-well plate and 200 μ*l* MTT solution were added to each well at the end of the predetermined time. The scaffolds were allowed to incubate in the dark at 37 °C for 4 h and MTT reagent was removed. 200 μ*l* of isopropanol/HCl mixture was added to the wells to dissolve the formazan reaction products. The color developed dye (100 μ*l*) from each well was pipetted out in 96-well plate for spectrophotometric analysis and the optical density (OD) of formazan solution was read on a microplate reader (Biochrom Asys Expert Plus. Microplate Reader, USA) at 570 nm.

The morphology and adhesion of HUVECs on the PU nanofibrous scaffolds were observed by SEM (JEOL JSM700F). Cells were cultured on the samples for 3 days at 37 °C (5 % CO_2). After 3 days of cell seeding, the cell-cultured PU scaffolds were prepared for SEM studies. The scaffolds were fixed in 4 % paraformaldehyde at room temperature for 30 min and then rinsed twice with PBS and dehydrated with upgrading concentrations of ethanol (60 %, 70 %, 80 %, 90 % and 100 %). Finally, the specimens were mounted on aluminum stubs and sputter coated with a mix of Au/Pt to observe the HUVECs cell morphology.

Cell Viability Analysis

HUVEC cells were cultured on PU nanofibrous scaffolds at a density of 5×10^3 cells/scaffolds and grew overnight. After 24 h incubation, the cell culture medium was removed and the cells were incubated with propodium iodide (PI) for 10 minutes at room temperature. The fluorescent images of five random fields in each well were taken by Fluorescence Inverted Microscope (Leica, Germany) including Texas Red® and FITC filters.

Hemolysis Assay

An ideal vascular graft should be blood compatible to mimic the endothelium. For the hemolysis assay, the bare and composite PU scaffolds were cut into small pieces and subjected to a hemolysis assay as per ISO 10993-4. Human blood was collected into a 3.8 % sodium citrate-coated tube from a healthy volunteer and diluted with PBS (pH 7.4) at a ratio of 100:1 (PBS/blood; v/v). Positive and negative controls were produced by adding 100 μ*l* of the blood to 10 m*l* of distilled water and PBS, respectively. The sterilized bare and composite PU scaffolds were immersed in a mixture of PBS and blood (100:1, v/v) and the samples were kept at 37 °C for 60 min. Then, the samples were centrifuged at 2,000 rpm for 10 min. The optical density (OD) of the supernatant was measured at 545 nm using a spectrophotometer (Biochrom Asys Expert Plus. Microplate Reader, USA) and the hemolysis percentage was calculated using the following equation:

$$HP(\%) = (OD_S - OD_{NC})/(OD_{PC} - OD_{NC}) \times 100$$

where, OD_S is the absorbance of a test sample, OD_{NC} is the absorbance of the negative control and OD_{PC} is the absorbance of the positive control. Each sample was studied three times.

Total Protein Measurement

Total protein content of the cell lysates was measured with the Bradford assay (Amresco, OH, USA). The absorbance of the solution was measured at 750 nm using a spectrophotometer (V-650 spectrophotometer, Jasco, Japan). The absorbance was then converted to protein content, as mg/m*l* using a bovine serum albumin standard curve.

Statistical Analysis

All data were expressed as mean±standard deviation of three independent experiments. Standard analysis of variance technique (ANOVA) was used to evaluate the statistical analysis of data. A *P*-value of less than 0.005 and 0.05 was considered statistically significant.

Results

Characterizations

An SEM micrograph of electrospun randomly-oriented bare and composite PU scaffolds is shown in Figure 1. The fibrous scaffolds consist of fibers with diameters ranging from 250 nm to 950 nm. The mean fiber diameters were 573±146 nm, 680±126 nm and 648±160 nm corresponding to the bare PU, PU-PEG, PU-PC, respectively. As can be seen in the SEM images, randomly-oriented scaffolds were highly uniform and had smooth nanofibers without the occurrence of bead defects.

Figure 2 showed the successful alignment of PU nanofibers. These photographs demonstrated that significant changes of the fiber morphology at aligned bare and composite PU scaffolds have been observed when the rotating mandrel was used. The PU, PU-PEG and PU-PC fiber diameters were at 546±186 nm, 758±190 nm and 447±145 nm, respectively. There is no statistical difference between ramdomly-oriented and aligned PU scaffolds fiber diameters. The bare PU and PU-PC aligned scaffold showed irregular pores between neighbored fibers caused by the intertwined and tortuous structure of the aligned fibers while PU-PEG scaffold presents a large surface area-to-volume ratio and interconnected porosity as well as a smooth surface and uniform diameters along its length.

FTIR analysis was carried out to determine the interactions among PU polymer chain, PEG and PC. Figure 3 shows the FTIR spectra of bare PU, PU-PEG, PU-PEG after immersion in water and PU-PC nanofiber scaffolds. For bare PU nanofibrillar scaffolds, the peak at 3326 cm^{-1} corresponded to the stretching ν(N-H). The peaks at 2940 and 2857 cm^{-1} were CH_2 peaks of the polyether, which corresponded to the asymmetric stretching and the symmetric stretching of CH_2, respectively. The peak was due to carbonyl groups and the C-N bonds were at 1731 cm^{-1} and 1525 cm^{-1}. The peak at 1415 cm^{-1} and the 1220 cm^{-1} were attributed to the symmetry bending vibration peak of -CH_2- and the ester C-O-C stretching in the PU segment, respectively. The obtained peaks were confirmed by the original peaks observed for PU in the literature [28,29].

The C-O-C stretching and O-H bending vibration peaks of PEG at 1099 cm^{-1} and 1342 cm^{-1} were clearly seen in Figure 3. These characteristic peaks of the PEG molecules strongly

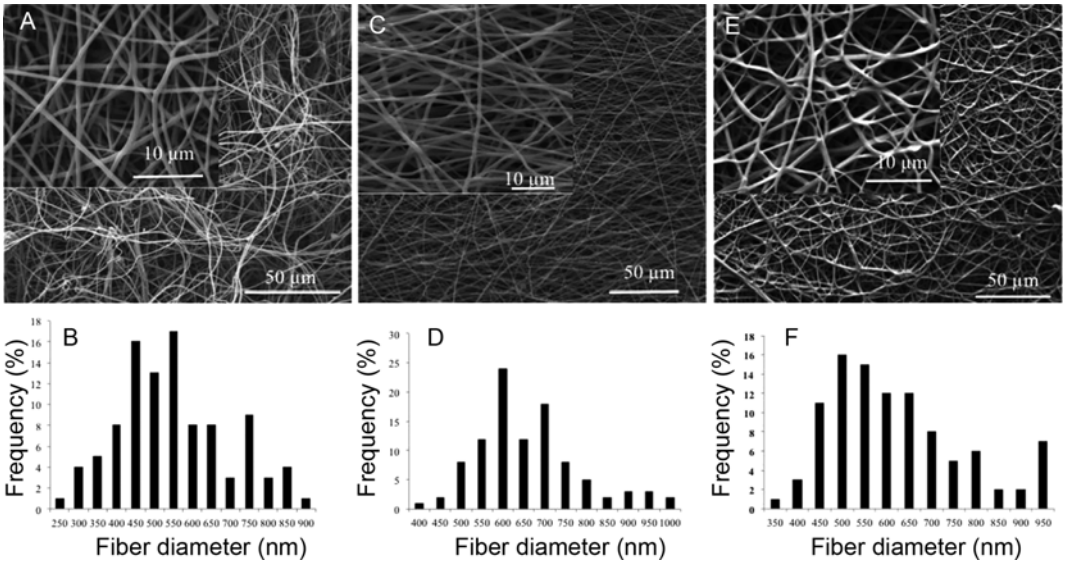

Figure 1. Surface morphology observed by SEM and the diameter distribution of randomly-oriented (A, B) bare PU; (C, D) PU-PEG and (E, F) PU-PC nanofiber scaffolds. Inset: close-up view of the nanofibers. 250 fibers for each sample were totally counted from five SEM images using ImageJ software, NIST.

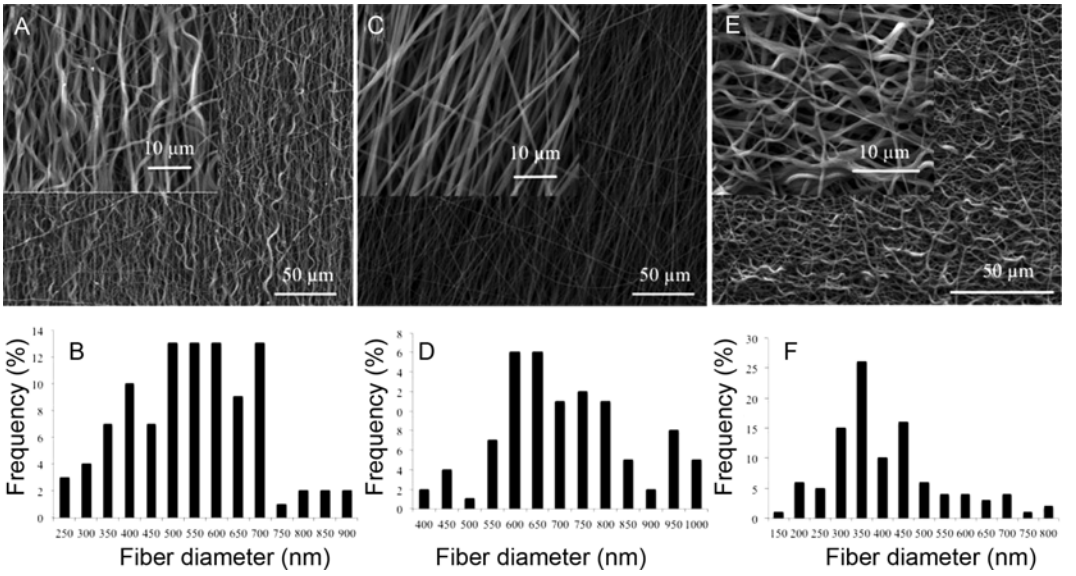

Figure 2. Surface morphology observed by SEM and the diameter distribution of aligned (A, B) bare PU, (C, D) PU-PEG and (E, F) PU-PC nanofiber scaffolds. Inset: close-up view of the nanofibers. 250 fibers for each sample were totally counted from five SEM images using ImageJ software, NIST.

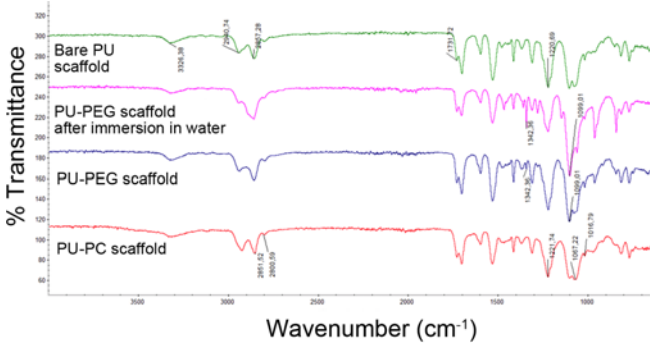

Figure 3. FTIR spectra of bare PU, PU-PEG, PU-PEG after immersion in water and PU-PC nanofiber scaffolds.

evidenced that composite PU-PEG scaffolds were successfully fabricated [28]. Furthermore, these observed bonds appeared completely proving the presence of PEG after continuous immersion in water of a few days.

After blending of PU with PC, the obtained spectrum at 2800 and 2851 cm^{-1}, 1221 and 1067 cm^{-1}, 1016 cm^{-1} belong to C-H stretching, PO_2 and CO-O-C groups. The obtained spectrums are similar to the bands of PC in the literature [30].

The contact angle between the PU scaffolds and the deionized water solution was measured to determine the wettability of nanofibrillar vascular grafts. The measured contact angle values of bare PU, PU-PEG and PU-PC are shown in Figure 4. As seen from Figure 4, the contact angles of the randomly-oriented and aligned bare PU nanofiber scaffold are about 122.3±0.86 ^{o} and 115.1±0.624 ^{o}, indicating that both the random and aligned scaffold surfaces are hydrophobic. The water droplet cannot spread well on the hydrophobic bare PU nanofiber scaffold surface, which is a disadvantage for cell spreading and proliferation. After the PEG or PC was combined with PU, the water droplet was immediately absorbed into the fibrous networks and the contact angle decreased gradually. With PC content, randomly oriented and aligned PU-PC scaffolds are quite hydrophilic with contact angle of 40.6±0.8 ^{o} and 39.1±0.8 ^{o}.

The mechanical properties of PU nanofibrous scaffolds were evaluated by tensile testing. The stress-strain curves of the samples are shown in Figure 5. As shown in this figure, the tensile strength of randomly-oriented PU nanofibers was 5.30±0.62 MPa and the elastic modulus was 2.97±0.79 MPa. By the addition of PEG and PC, tensile strength increased to 7.23±0.72 MPa and 7.59±0.80 MPa with an elastic modulus of 68.82±19.80 MPa and 2.20±0.06 MPa, respectively (Table 1).

MTT Assay

The time dependent-cellular adhesion and -proliferation were indirectly studied by MTT assay. The MTT assay was used to measure the OD of formazan-containing media. The yellow tetrazolium salt is reduced to purple formazan crystals in metabolically active cells. The absorbance obtained from formazan crystals is proportional to the number of viable cells. Statistical analysis of data showed that the difference between viable cells on the random-oriented, aligned bare PU and the aligned PU-PC nanofiber scaffold is significant at the end of day 7 ($p<0.005$). Furthermore, the obtained absorbance revealed greater cell attachment and spreading in

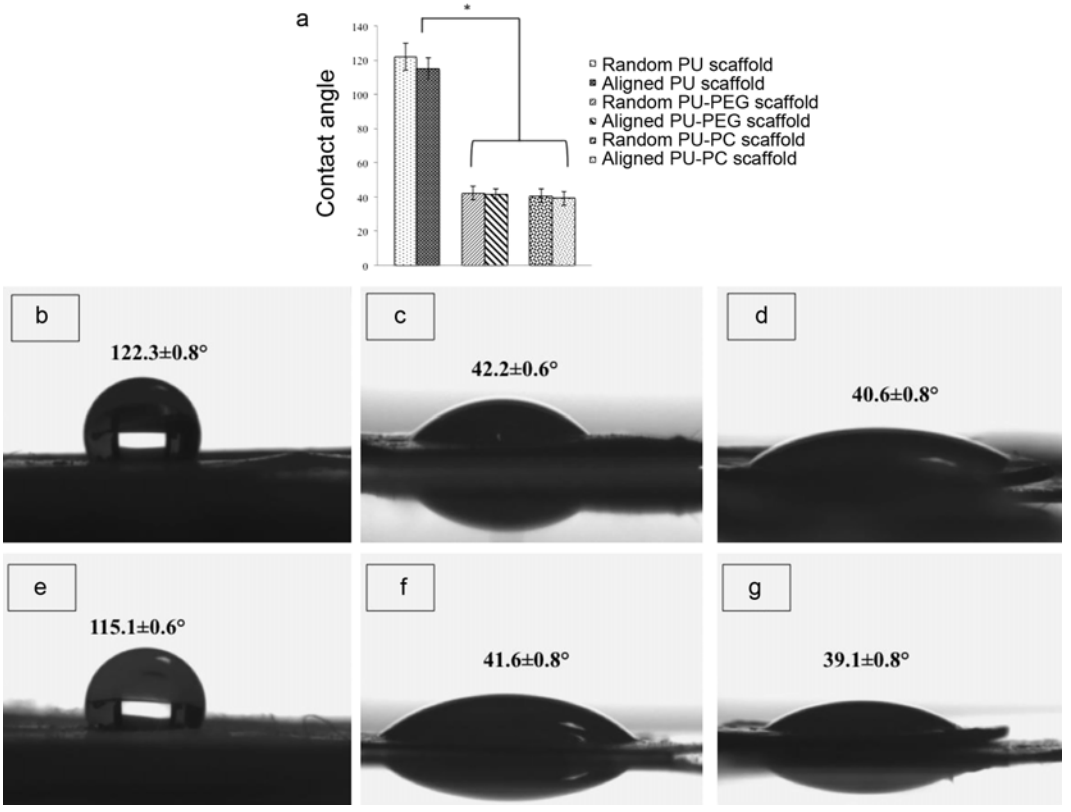

Figure 4. (a) Comparison of water contact angle values for the randomly-oriented and aligned nanofiber scaffolds. Images of the water contact angles for the randomly-oriented (b) bare PU, (c) PU-PEG, (d) PU-PC and aligned (e) bare PU, (f) PU-PEG, (g) PU-PC nanofiber scaffolds. Values are mean +/− SEM; n=5; *p<0.005, compared to the bare and aligned PU nanofiber scaffolds.

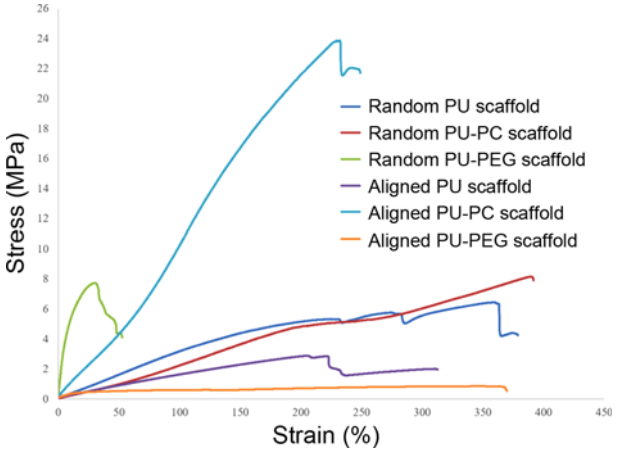

Figure 5. Stress-strain curves of randomly-oriented and aligned bare PU, PU-PEG and PU-PC nanofiber scaffolds.

the aligned PU-PEG scaffolds as compared with the bare PU scaffolds ($p<0.05$) (Figure 6).

The adhesion of HUVECs on PU scaffolds was observed using scanning electron microscopy in Figure 7. SEM images showed that HUVECs tend to spread more on the PU-PC aligned nanofiber scaffold and support cell adhesion and proliferation as well as aligned PU-PEG nanofibrillar scaffolds. Photographs of HUVECs on electrospun nanofiber scaffolds showed normal cell morphology and the cells spread to the PU scaffolds with bipolar and tripolar extensions. However, as it is observed from SEM images, there are not many cells adhered on bare PU nanofibrillar scaffolds.

Table 1. The mechanical properties of randomly-oriented and aligned bare PU, PU-PEG and PU-PC nanofiber scaffolds

	Tensile strength (MPa)	Elongation at break (%)	Modulus (MPa)
Random PU scaffold	5.30±0.62	331.12±67.62	2.97±0.79
Random PU-PEG scaffold	7.23±0.72	60.13±10.65	68.82±19.8
Random PU-PC scaffold	7.59±0.80	370.90±29.32	2.20±0.06
Aligned PU scaffold	3.22±0.47	318.78±8.50	2.00±0.22
Aligned PU-PEG scaffold	0.80±0.07	321.65±68.23	4.24±0.63
Aligned PU-PC scaffold	23.95±0.09	282.87±47.84	10.33±0.57

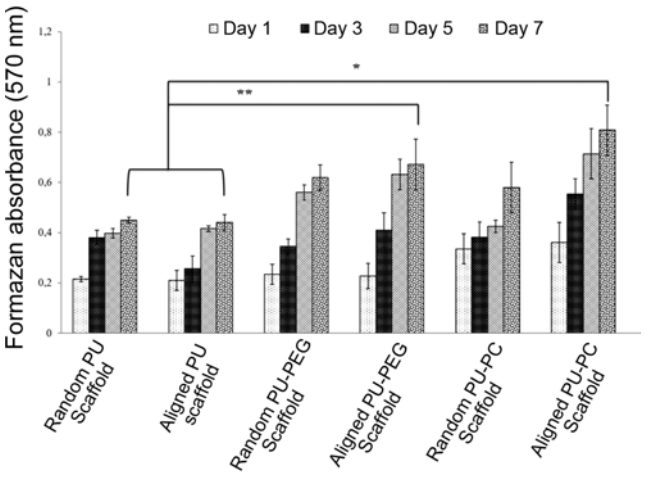

Figure 6. MTT results of HUVECs on the bare PU, PU-PEG and PU-PC nanofiber scaffolds. Values are mean +/− SEM; n=3. *p<0.005, **p<0.05 compared to the bare and aligned PU nanofiber scaffolds.

Cell Viability Analysis

The fluorescent images of the HUVEC cells after 24-hour exposure to the PU scaffolds were obtained. As shown in Figure 8, more dead HUVEC cells were observed on the randomly-oriented PU scaffolds. Furthermore, the aligned PU-PEG and PU-PC nanofiber scaffolds were more active than bare PU scaffolds. The improved activity could be interpreted as an influence of fiber alignment on cells. Conversely, it is clear from the Figure 7 and 8 that the HUVEC cells with aligned modified PU scaffolds showed lower dead cell ratio compared to bare and randomly-oriented forms.

Hemolysis Assay

The hemocompatibility of the bare and composite PU nanofibrillar scaffolds was evaluated by hemolysis test. The hemolysis percentage is an indicator of the extent of red blood cells broken by the scaffolds contacting with blood. The lower hemolysis percentage means the better the blood compatibility for the biomaterials. Figure 9 reflects the hemolysis percentage of the bare and composite PU scaffolds. Both PU-PEG and PU-PC nanofibrillar scaffolds have a hemolysis percentage less than that of the bare PU. Randomly-oriented PU-PEG showed the lowest value (0.48±0.5 %) (Figure 9).

Total Protein Measurement

Protein adsorption is an extremely unfavorable event during the interaction of blood with implanted biomaterials because of the subsequent biological responses including platelet adhesion and activation as well as bacterial adhesion.

Protein adsorption is a critical early event during the interaction of blood with implanted biomaterials, and mediates the subsequent biological responses including platelet adhesion and activation as well as bacterial adhesion.

The total protein synthesized by HUVECs cultured on PU scaffolds was determined using a standard absorbance curve of albumin and expressed in milligrams. Total protein

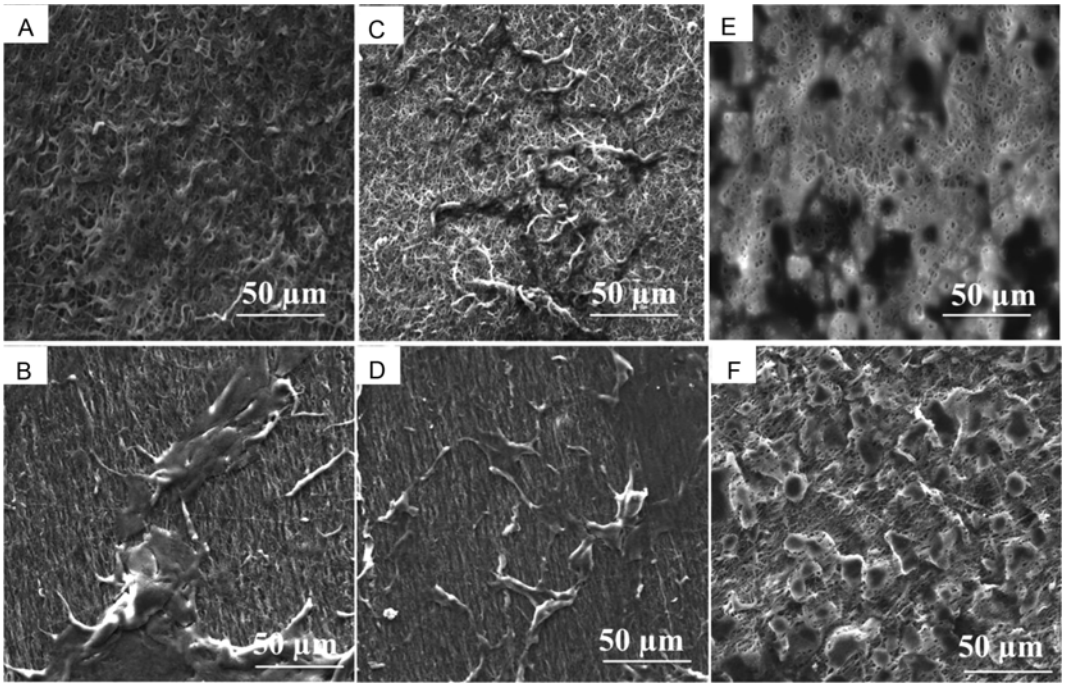

Figure 7. SEM images of HUVECs on the surface of the randomly-oriented and aligned bare PU (A, B), PU-PEG (C, D) and PU-PC (E, F) nanofiber scaffolds, respectively. Scale bars are 50 µm.

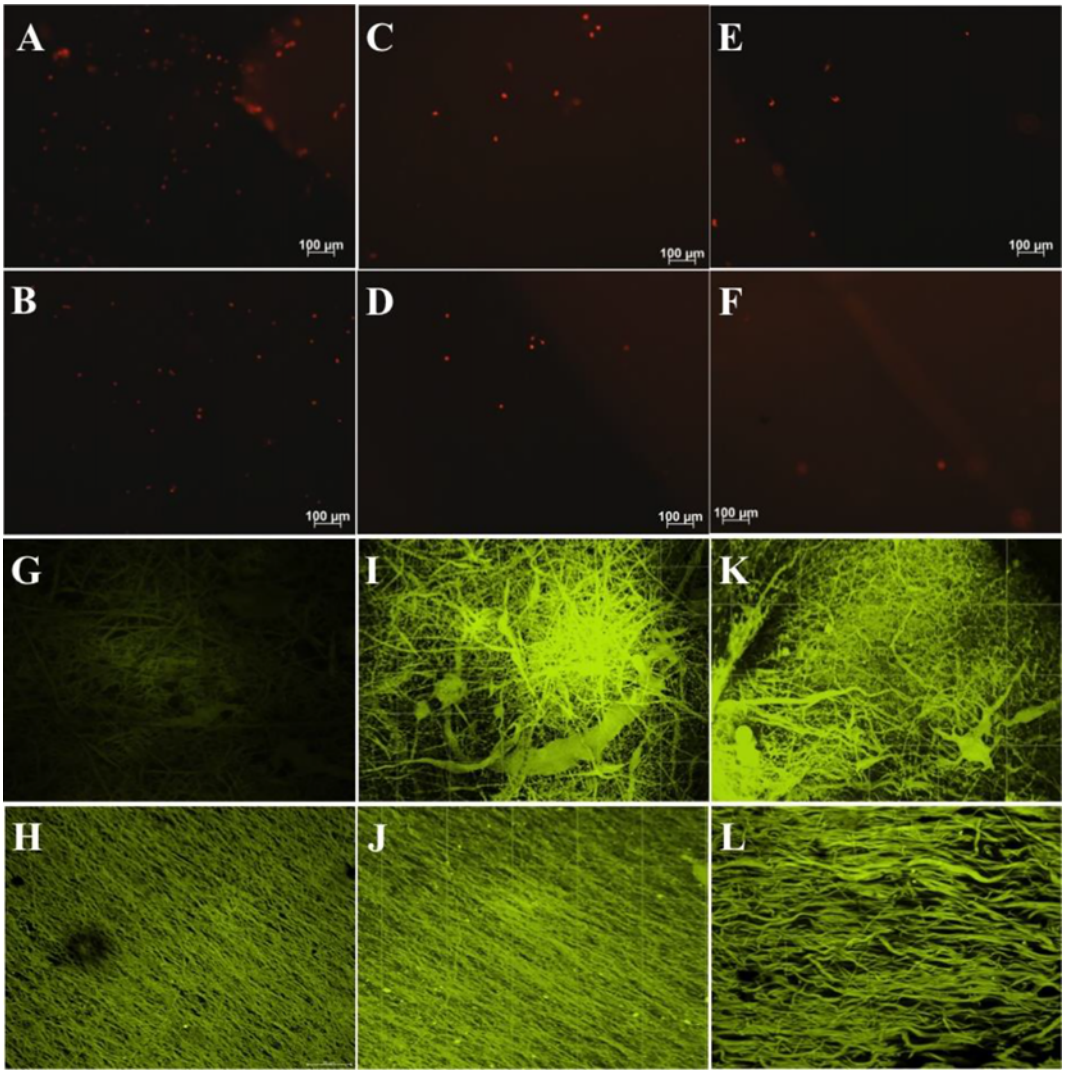

Figure 8. Fluorescence microscopy images of HUVEC cells after 24 h incubation with randomly-oriented and aligned bare PU (A, B), PU-PEG (C, D) and PU-PC (E, F) nanofiber scaffolds, respectively. Fluorescent images of randomly-oriented and aligned bare PU (G, H), PU-PEG (I, J) and PU-PC (K, L) nanofiber scaffolds. The dead cells are stained with PI, a red dye and the fibers are stained with Alexa Fluors 488, a green dye. Scale bars are 100 μm.

contents of cells were quantified at 1, 3, 5 and 7 days and the results are shown in Figure 10. As shown in Figure 10, all of the modified samples show more resistance in the adsorption of protein. Further studies revealed that super hydrophilic surfaces lead to a lower protein adsorption because of large repulsive forces produced on the proteins [31]. In this study, the reduction in adsorption of protein on PU-PEG surface was evidenced by the interaction forces between protein and surfaces and it suggesting that PEG is resistant to protein adsorption on randomly oriented or aligned PU surface. Furthermore, the bare PU electrospun scaffolds showed the highest protein adsorption compared to randomly-oriented or aligned PU-PC after 7 days of culture ($p<0.05$). Van der Heiden *et al*. reported that the highly ordered structure of natural phospholipid bilayers suppressed protein adsorption effectively [32]. Furthermore, Zhang *et al*. showed that fibrinogen adsorption on phosphatidylcholine (PC) polar headgroups-modified surface was decreased by 98 % to 87 % compared to that on ordinary polyurethane surfaces, and almost no platelet adhesion and activation was observed [33]. Herewith, it is believed that the PU-PEG or PU-PC nanofiber scaffolds demonstrate good potential for the development of surfaces with minimal thrombogenic character in *in vivo* applications.

Discussion

Herein, we developed a small diameter PU vascular graft

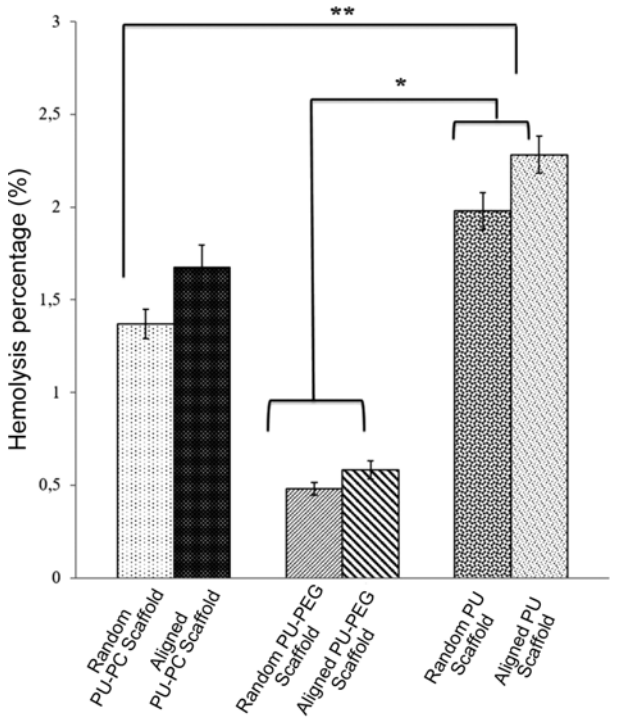

Figure 9. Hemolysis ratios of the randomly-oriented and aligned bare PU, PU-PEG and PU-PC nanofiber scaffolds. Values are mean +/− SEM; n=3. *p<0.005, **p<0.05 compared to the bare and aligned PU nanofiber scaffolds.

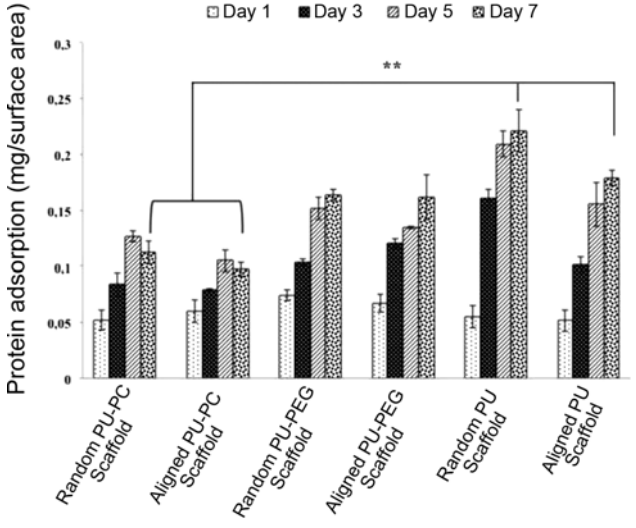

Figure 10. Total protein content of the randomly-oriented and aligned bare PU, PU-PEG and PU-PC nanofiber scaffolds. Values are mean +/− SEM; n=3. **p<0.05 compared to the bare and aligned PU nanofiber scaffolds.

with submicron randomly-oriented and aligned topography, which mimicked the tunica intima of the native arterial vessels. Natural lecithin (PC) and PEG molecules were combined with the hydrophobic PU by physical and chemical blending. These prepared blends were processed by electrospinning into randomly-oriented and aligned fibrous scaffolds. The type of collector used in the electrospinning process affects the morphology of the collected fibers. The SEM micrographs of random-oriented fibers show them to be highly uniform with diameters ranging from 200 nm to 900 nm. It was observed that the fiber diameter increased slightly after PEG and PC modifications. Llorens *et al*. reported that the fiber diameters of scaffolds comprising different ratios of poly(ethylene glycol) (PEG) and polylactide (PLA) electrospun fibers increased with a high PEG content [34]. Similarly, the diameters of PU nanofibers exhibited a little difference after PEG- or PC doping in this study. Furthermore, specifically, samples having a PC content showed a bonded fiber structure. In conclusion, it may be stated that the transition from beaded fibers to elongated fibers with chain entanglement increasement in the supramolecular structure [35].

FTIR analysis is used to investigate the intermolecular interaction among PU polymer chain, PEG and PC. The results indicate that the specific bands attributed to PU, PEG or PC appeared completely proving the presence of each component.

Appropriate surface energy of the surface would be conducive to cell attachment and proliferation. In this study, a small amount PEG or PC improved the hydrophilicity of electrospun PU scaffolds and the water contact angle of PU-PEG or PU-PC scaffolds decreased significantly due to the hydrophilicity of PEG or PC. Similar results have been reported in the literature [36,37]. Furthermore, considering the contact angle measurements, it was also proven that the fiber orientation did not significantly affect the surface wettability of PU nanofibrillar scaffolds [38].

An ideal scaffold should have enough mechanical strength to support growing tissue. The mechanical properties of PU-PEG- and PU-PC scaffolds are much higher than those of bare PU nanofibrillar scaffolds. However, as shown in Figure 5, compared with those of the bare randomly-oriented PU, the ultimate tensile properties of the aligned PU reduced as well as PU-PEG nanofiber scaffolds. Kim *et al*. developed a method to fabricate highly-aligned electrospun nerve guide conduit with selective permeability using various materials including poly lactic-co-glycolic acid (PLGA) and polyurethane (PU). According to mechanical testing results, the aligned nanofibrous mats also have a weaker mechanical strength relative to the randomly-oriented nanofibrous mat. A lower mechanical strength was observed in the aligned nanofibrous structures which may be related to the fewer contact points in the aligned nanofibers [39].

Ou *et al*. reported a nanocomposite of poly(lactic acid) reinforced with cellulose nanofibrils. In this study, PEG was added to the matrix as a compatibilizer to improve the interfacial interaction between the hydrophobic poly(lactic acid) (PLA) and the hydrophilic cellulose nanofibrils and

they found that the addition of PEG to the blend of PLA resulted in significant improvement in percentage elongation (25 %) compared to pure PLA [40]. However, the randomly PU-PEG nanofibers showed low elongation at break compared to the other counterparts due to their plasticizing or hardening effect [36]. In this study, with the addition of the hydrophilic block, PEG, both the modulus and strain at maximum load decreased for both forms, i.e. randomly-oriented and aligned PU nanofibers. The obvious differences of mechanical properties between bare PU and PU/PEG hybrid scaffolds resulted from different molecular masses of PEG having different effects on the thermal and mechanical behavior of the scaffolds. Fray *et al*. found that terpolymers with PEG1000 showed low tensile strength and elongation at break and the stress-strain curve shapes [41]. Furthermore, inter-molecular interaction at the soft segment sites is reduced as the molecular weight increases, and this may also be responsible for the early break of the PU-PEG [42].

In addition to that, the aligned PU/PC nanofibers significantly increased the mechanical properties of the nanofibrous scaffold. For example, the tensile strength and elastic modulus were 5-fold that of the PU randomly-oriented group. A similar result is reported by Harini *et al.* [43]. They developed an electrospun polycaprolactone (PCL) membrane loaded with egg lecithin and terbinafine hydrochloride (terbinafine) against moulds and dermatophytic fungi and they investigated their effect on mechanical properties, swellability, cell adhesion, biocompatibility and photoluminescence properties. The mechanical analysis showed that the ultimate tensile stress of PCL/Lec increased with the incorporation of lecithin content.

As reported in the literature, a decellularized pig femoral artery has shown an average tensile strength of 3.4 MPa and an average tensile modulus of 2.7 MPa [44]. These results indicated that the mechanical properties of the randomly-oriented PU-PEG and aligned PU-PC are closer to those of pig arteries.

In this study, we hypothesized that increased hydrophilicity by the blending of PC and PEG will promote HUVECs attachment and proliferation. The results showed that the cells attached, survived and proliferated on the PU-PEG- and PU-PC scaffolds significantly better compared with the bare PU scaffolds. PEG and PC-reinforcement generally create a more hydrophilic surface on PU scaffolds. In contrast, the bare PU nanofiber scaffold is hydrophobic as shown in contact angle results. Previous literature reports that cellular adhesion improves with hydrophilicity [45].

The hemocompatibility of biomaterials is an important factor for vascular tissue engineering applications. An ideal synthetic polymeric vascular scaffold should appropriate physicochemical properties to prevent thrombogenicity and secondary infection. In this study, the lecithin-reinforced electrospun scaffolds displayed a not much higher hemolysis percentage than PU-PEG scaffolds. This can be explained through the non-thrombogenic property of natural lecithin [46]. The positive effect of PEG on blood cell adhesion and hemocompatibility was reported in previous studies [37,47]. In general, these results indicate that both PU-PC and PU-PEG electrospun scaffolds exhibit good blood biocompatibility and may be developed as a substitute for small-diameter blood vessels in clinic. Furthermore, the total amount of protein adsorbed was found to decrease with blending of scaffolds using PEG or PC. Therefore, the obtained results provide a meaningful data to determine biological response to materials of PEG and PC-blending.

Conclusion

In this study, a new strategy was developed for vascular tissue regeneration by modifying of PU nanofibrillar scaffolds using PEG and PC to promote cell and blood biocompatibility. We successfully fabricated nanofibrous PU scaffolds blended by PEG and PC to promote HUVECs survival. The scaffold morphology maintained the original structure very well and the average diameter of the fibers did not change significantly after blending. The PEG or PC hybrid scaffolds showed higher hydrophilicity, lower hemolysis than PU scaffolds. Furthermore, HUVECs attached well on the PEG or PC hybrid fibrous scaffolds. Based on these results, we suggest that the nanofibrous scaffolds with oriented nanofibers fabricated through combining PU with the hydrophilic PEG and PC could provide a potential substitute for small-diameter vascular graft.

Acknowledgments

The authors would like to thank Dr. Murat Demirbilek for technical support in mechanical tests and biocompatibility assays.

References

1. World Health Organization, Fact Sheet No, **317**, 2012.
2. D. Mozaffarian, E. J. Benjamin, A. S. Go, D. K. Arnett, M. J. Blaha, M. Cushman, S. de Ferranti, J. P. Despres, H. J. Fullerton, V. J. Howard, M. D. Huffman, S. E. Judd, B. M. Kissela, D. T. Lackland, J. H. Lictman, L. D. Lisabeth, S. Liu, R. H. Mackey, D. B. Matchar, D. K. McGuire, E. R. Mohler, C. S. Moy, P. Muntner, M. E. Mussolino, K. Nasir, R. W. Neumar, G. Nichol, L. Palaniappan, D. K. Pandey, M. J. Reeves, C. J. Rodriquez, P. D. Sorlie, J. Stein, A. Towfighi, T. N. Turan, S. S. Virani, J. Z. Willey, D. Woo, R. W. Yeh, and M. B. Turner, *Circulation*, **131**, 329 (2015).
3. L. E. Niklason and R. S. Langer, *Transpl. Immunol.*, **5**, 303 (1997).
4. E. R. Edelman, *Circ Res.*, **85**, 1115 (1999).
5. L. Bordenave, P. Menu, and C. Baquey, *Expert. Rev. Med. Dev.,* **5**, 337 (2008).

6. A. Rathore, M. Clear, Y. Naito, K. Rocco, and C. Breuer, *Wiley Interdiscip Rev. Nanomed Nanobiotechnol.*, **4**, 257 (2012).
7. M. D. Lelah and S. L. Copper, "Polyurethane in Medicine", Boca Raton, FL, USA: CRC Press, 1987.
8. A. Burke and N. Hasirci, *Adv. Exp. Med. Biol.,* **553**, 83 (2004).
9. T. Hentschel and H. Munstedt, *Infection,* **27**, S43 (1999).
10. T. Matsuda, M. Ihara, H. Inoguchi, I. K. Kwon, K. Takamizawa, and S. Kidoaki, *J. Biomed. Mater. Res. A.,* **73A**, 125 (2005).
11. J. J. Stankus, L. Soletti, K. Fujimoto, Y. Hong, D. A. Vorp, and W. R. Wagner, *Biomaterials*, **28**, 2738 (2007).
12. M. R. Williamson, R. Black, and C. Kielty, *Biomaterials,* **27**, 3608 (2006).
13. L. Soffer, X. Wang, X. Zhang, J. Kluge, L. Dorfmann, D. L. Kaplan, and G. Leisk, *J. Biomater. Sci. Polym. Ed.,* **19**, 653 (2008).
14. M. Li, M. J. Mondrinos, X. Chen, M. R. Gandhi, F. K. Ko, and P. I. Lelkes, *J. Biomed. Mater. Res. A.,* **79**, 963 (2006).
15. C. M. Vaz, S. van Tuijl, C. V. Bouten, and F. P. Baaijens, *Acta Biomater.,* **1**, 575 (2005).
16. F. M. Ballarin, P. C. Caracciolo, E. Blotta, V. L. Ballarin, and G. A. Abraham, *Mater. Sci. Eng. C. Mater.,* **42**, 489 (2014).
17. K. K. Sankaran, K. S. Vasanthan, U. M. Krishnan, and S. Sethuraman, *J. Tissue Eng. Regen Med.,* **8**, 640 (2014).
18. M. J. McClure, S. A. Sell, D. G. Simpson, B. H. Walpoth, and G. L. Bowlin, *Acta Biomater.,* **6**, 2422 (2010).
19. A. K. Gaharwar, M. Nikkhah, S. Sant, and A. Khademhosseini, *Biofabrication,* **7**, 015001 (2014).
20. H. Wang, Y. Feng, Z. Fang, W. Yuan, and M. Khan, *Mater. Sci. Eng: C.,* **32**, 2306 (2012).
21. H. Wang, Y. Feng, B. An, W. Zhang, M. Sun, Z. Fang, W. Yuan, and M. Khan, *J. Mater Sci: Mater Med.,* **23**, 1499 (2012).
22. X. Zhang, D. Tan, J. Li, H. Tan, and Q. Fu, *Biofuling,* **27**, 919 (2011).
23. D.-L. Fang, Y. Chen, B. Xu, K. Ren, Z.-Y. He, L.-L. He, Y. Lei, C.-M. Fan, and X.-R. Song, *Int. J. Mol. Sci*., **15**, 3373 (2014).
24. X. Su, Z. Wang, L. Li, M. Zheng, C. Zheng, P. Gong, P. Zhao, Y. Ma, Q. Tao, and L. Cai, *Mol. Pharm*., **10**, 1901 (2013).
25. L. Liu, C. Zhou, X. Xia, and Y. Liu, *Int. J. Nanomedicine,* **11**, 761 (2016).
26. J. Cao, N. Chen, Y. Chen, and X. Luo, *Int. J. Mol. Sci.,* **26**, 1870 (2010).
27. R. Nirmala, H. M. Park, R. Navamathavan, H. S. Kang, M. H. El-Newehy, and H. Y. Kim, *Mater. Sci. Eng: C.,* **31**, 486 (2011).
28. V. Chiono, P. Mozetic, M. Boffito, S. Sartori, E. Gioffredi, A. Silvestri, A. Rainer, S. M. Giannitelli, M. Trombetta, D. Nurzynska, F. D. Meglio, C. Castaldo, R. Miraglia, S. Montagnani, and G. Ciardelli, *Interface Focus*., **4**, 20130045 (2013).
29. R. C. M. Dias, A. M. Góes, R. Serakides, E. Ayres, and R. L. Oréfice, *Mater. Res.,* **13**, 211 (2010).
30. J. M. Nzai and A. Proctor, *J. Am. Oil Chem. Soc.,* **76**, 61 (1999).
31. J. Zheng, L. Li, H.-K. Tsao, Y.-J. Sheng, S. Chen, and S. Jiang, *Biophys. J*., **89**, 158 (2005).
32. A. P. van der Heiden, G. M. Willems, T. Lindhout, A. P. Pijpers, and L. H. Koole, *J. Biomed. Mater. Res.*, **40**, 195 (1998).
33. X. Zhang, D. Tan, J. Li, H. Tan, and Q. Fu, *Biofouling*, **27**, 919 (2011).
34. E. Llorens, S. Bellmunt, L. J. del Valle, and J. Puiggali, *J. Polym. Res.,* **21**, 603 (2014).
35. M. G. McKee, J. M. Layman, M. P. Cashion, and T. E. Long, *Science,* **311**, 353 (2006).
36. H. Wang, Y. Feng, H. Zhao, Z. Fang, M. Khan, and J. Guo, *J. Nanosci. Nanotechnol.,* **13**, 158 (2013).
37. H. Shi, H. Liu, S. Luan, D. Shi, S. Yan, C. Liu, R. K. Y. Li, and J. Yin, *RSC Adv.,* **6**, 192388 (2016).
38. H. Jahani, S. Kaviani, M. Hassanpour-Ezatti, M. Solelmani, Z. Kaviani, and Z. Zonoubi, *Cell J.,* **14**, 31 (2012).
39. J. I. Kim, T. I. Hwang, L. E. Aguilar, C. H. Park, and C. S. Kim, *Sci. Rep*., **29**, 23761 (2016).
40. P. Qu, Y. Gao, G. Wu, and L. Zhang, *BioResources*, **5**, 1811 (2010).
41. M. El Fray and H. D. Wagner, *Des. Monomers Polym.*, **15**, 547 (2012).
42. J. W. Cho, Y. C. Jung, Y. C. Chung, and B. C. Chun, *J. Appl. Polym. Sci.*, **93**, 2410 (2004).
43. S. Harini, M. Venkatesh, S. Radhakrishnan, M. H. U. T. Fazil, E. T. L. Goh, S. Rui, C. Dhand, S. T. Ong, V. A. Barathi, R. W. Beuerman, S. Ramakrishna, N. K. Verma, and R. Lakshminarayanan, *RSC Advances*, **6**, 41130 (2016).
44. M. McClure, S. A. Sell, C. P. Barnes, W. C. Bowen, and G. L. Bowlin, *J. Eng. Fibers Fabrics.,* **3**, 1 (2008).
45. K. Geunhyung and K. Wandoo, *J. Biomed. Material. Res. B: Appl. Biomater.,* **81B**, 104 (2007).
46. M. Zhang, K. Wang, Z. Wang, B. Xing, Q. Zhao, and D. Kong, *J. Mater. Sci. Mater. Med.,* **23**, 2639 (2012).
47. T. Nakaya and Y. J. Li, *Prog. Polym. Sci.,* **24**, 143 (1999).